Applied Geography 63 (2015) 315–325

Contents lists available at ScienceDirect

Applied Geography

journal homepage: www.elsevier.com/locate/apgeog

Extracting ecological information from oblique angle terrestrial landscape photographs: Performance evaluation of the WSL Monoplotting Tool☆

Christopher A. Stockdale [a, *], Claudio Bozzini [b], S. Ellen Macdonald [a], Eric Higgs [c]

[a] Department of Renewable Resources, Faculty of Agriculture, Life and Environmental Science, University of Alberta, 743 General Services, Edmonton, Alberta, T6G 2H1, Canada
[b] Insubric Ecosystem Research Group, Swiss Federal Institute for Forest, Snow and Landscape Research WSL, Bellinzona, Switzerland
[c] School of Environmental Studies, University of Victoria, Victoria, British Columbia, Canada

ARTICLE INFO

Article history:
Received 7 May 2015
Received in revised form
20 July 2015
Accepted 21 July 2015
Available online xxx

Keywords:
Georeferencing oblique photographs
Repeat photography
Alberta Rocky Mountains
Mountain Legacy Project
Ecosystem change
WSL Monoplotting Tool
Photogrammetry
Remote sensing

ABSTRACT

While aerial photography and satellite imagery are the usual data sources used in remote sensing, land based oblique photographs can also be used to measure ecological change. By using such historical photographs, the time frame for change detection can be extended into the late 1800s and early 1900s, predating the era of aerial imagery by decades. Recent advancements in computing power have enabled the development of techniques for georeferencing oblique angle photographs. The WSL Monoplotting Tool is a new piece of software that opens the door to analyzing such photographs by allowing for extraction of spatially referenced vector data from oblique photographs. A very large repeat photography collection based on the world's largest systematic collection of historical mountain topographic survey images, the Mountain Legacy Project, contains >6000 high resolution oblique image pairs showing landscape changes in the Rocky Mountains of Alberta between ca. 1900 – today. We used a subset of photographs from this collection to assess the accuracy and utility of the WSL Monoplotting Tool for georeferencing oblique photographs and measuring landscape change. We determined that the tool georeferenced objects to within less than 15 m of their real world 3D spatial location, and the displacement of the geographic center of over 121 control points was less than 3 m from the real world spatial location. Most of the error in individual object placement was due to the angle of viewing incidence with the ground (i.e., low angle/highly oblique angles resulted in greater horizontal error). Simple rules of control point selection are proposed to reduce georeferencing errors. We further demonstrate a method by which raster data can be rapidly extracted from an image pair to measure changes in vegetation cover over time. This new process permits the rapid evaluation of a large number of images to facilitate landscape scale analysis of oblique imagery.

1. Introduction

Being able to measure and document ecosystem and landscape change through time contributes to our understanding ecological dynamics, historical ecology, environmental management and ecological restoration (Higgs et al. 2014). Numerous studies using widely varied methodologies have shown that across western North America, grasslands and open canopy forests have been lost to encroachment and densification of forests over the last century (Arno & Gruell, 1983; Gruell, 1983; Baker, 1992; Rhemtulla, Hall, Higgs, & Macdonald, 2002). These changes are believed to have caused decreased landscape vegetation diversity (Shinneman, Baker, Rogers, & Kulakowski, 2013; Romme et al. 2009), and increased the susceptibility of forests to wildfire (Baker, 1992; Agee, 1998) and biotic disturbances (Arno, Parsons, & Keane, 2000). We need to be able to measure ecosystem change over a relevant time period and spatial resolution to inform management needs and enhance planning efforts designed to mitigate these ecological problems.

Remote sensing can measure changes in patterns, but is limited

☆ WSL – Abbreviation for the Swiss Federal Institute for Forest, Snow and Landscape Research.

* Corresponding author.
E-mail address: cstockda@ualberta.ca (C.A. Stockdale).

http://dx.doi.org/10.1016/j.apgeog.2015.07.012
0143-6228/

to the recent past: in most of North America the earliest aerial photography dates to the 1930s, and in the region of western Canada we study, the first systematic aerial survey was conducted in 1949. To look further back in time, some researchers have used historical land based oblique angle photographs (as old as 1870s) to describe ecosystem change. Hastings and Turner (1965), Gruell (1980; 1983), and Webb (1996) have all used historical repeat photography to describe ecological changes over periods of 80–100 years. Some of these studies predated the development of Geographic Information Systems (GIS) software, which limited their ability to conduct spatial analyses. Hastings and Turner (1965) were limited to purely descriptive measures showing changes in the natural vegetation of arid and semi-arid areas. Gruell (1980; 1983) was also limited to using repeat photography for purely descriptive purposes to show the scale of vegetation change in Montana and Idaho between 1871 and 1982. He described in detail the changes in vegetation type, fire frequency, and processes such as snag fall but lacked any quantitative or spatial measurements. Webb (1996), like previous investigators, was able to describe changes in vegetation type, and changes in river flow patterns, but was limited by the inability to spatially reference the images and quantify these changes.

For repeat-photograph studies done using GIS, the challenges associated with georeferencing oblique angle photographs limited the analyses to describing changes qualitatively. Attempts at quantitative assessments of historical photographs by labor intensive manual procedures have been limited to the small spatial scale of only a few meadows (Roush, Munroe, & Fagre, 2007) or single valleys (Rhemtulla et al. 2002; Watt-Gremm, 2007). Rhemtulla et al. (2002) used repeat photography to document 80 years of vegetation change in the montane regions of Jasper National Park, Alberta, Canada. These images are part of the Mountain Legacy Project (Higgs, Bartley, & Fisher, 2009) collection, and image pairs were adjusted to enable accurate overlays. Changes in vegetation type were noted at each pixel, but due to changing scale within the images (foreground pixels representing less area than background pixels) this only revealed relative rather than absolute measures of change. Their assessment was limited to 20 pairs of photographs, covering a total area of approximately 6000 ha.

Manier and Laven (2002) used remote sensing classification techniques to detect change in vegetation using historical photographs spanning 80–100 years, but their comparisons between the two time periods were restricted to relative changes such as relative percent cover, relative patch size and the number of patches by vegetation type.

Roush et al. (2007) used a grid overlay in a GIS to evaluate change in repeat photographs in Glacier National Park, Montana, USA, but the grid was of a constant size overlain on the images. Grid cells over vegetation in the image foreground represented less area than grid cells over vegetation in the background of the image. Their study was detailed in relative change measures, but no spatial measurements were obtained.

Watt-Gremm (2007) used the Mountain Legacy images to examine vegetation change in the Blakiston Valley of Waterton Lakes National Park, Alberta, Canada. In an effort to make the change measurements spatial, he used a GIS to create a spatial grid, drape it on a DEM of the study area, manually rotate the view of the draped grid to match the photo perspective as closely as possible, and overlay it on the image in Photoshop to classify the vegetation in each grid cell. The process used by Watt-Gremm inspired the development of the raster analysis method described below in this paper. However, Watt-Gremm did all of this manually, and thus was limited to analyzing only seven image pairs, covering less than 2000 ha in total, and the accuracy is unknown because the perspective-rotated grid overlain on the image was not analyzed in a GIS.

As the above-mentioned researchers were beginning to make use of historical photographs, and working on methods to quantify change, they all noted the challenges associated with spatially referencing land based oblique images. Early attempts to create computer based methods for spatially referencing oblique-angle photographs (Aumann & Eder, 1996; Aschenwald, Leichter, Tasser, & Tappeiner, 2001; Mitishita, Machado, Habib, & Gonçalves, 2004; Corripio, 2004; Fluehler, Niederoest, & Akca, 2005) have not been widely adopted because they are task-specific, relatively inaccurate, and were restricted by available computing power. Corripio (2004) developed a computer program that georeferenced oblique images by allowing the user to manually rotate a DEM to a perspective matching an oblique image. The user inserts control points on the image, and visually aligns these control points with the same marks on the DEM. For small areas, and when working with very few photographs, this system functions as intended, however it takes considerable trial and error to get the alignment correct. The image is then rubbersheeted and can be viewed in a GIS. Watt-Gremm (2007), Roush et al. (2007), Bozzini, Conedera, and Krebs (2012), and this author have all used the Corripio (2004) application, and while it worked for its intended purpose, all of these researchers found it is very difficult to orient the camera correctly to obtain an accurately georeferenced rubbersheeted image.

Considering the aforementioned challenges associated with quantifying changes visible in terrestrial oblique angle images, no one has yet used historic photographs to conduct a landscape-level (100's–1000's km^2) quantitative assessment of vegetation pattern change across a century. With a growing number of historical photograph collections that can be used to measure historical landscape change, developing accurate methods to analyze these images within a GIS would be of great benefit. One such collection is the Mountain Legacy Project (MLP) (Trant, Starzomski, & Higgs, 2015; Higgs et al. 2009), which has collected images in Canada from the 1870's to 1950's. Of nearly 140,000 historical oblique angle photographs, 4500 photographs have been retaken since the late 1990s, with repeat photography ongoing. The majority of these photo pairs are of the landscape of the Alberta Rocky Mountains and foothills region (see Fig. 1).

Recently, Bozzini et al. (2012) developed a new method of georeferencing oblique photographs to extract vector data: the WSL Monoplotting Tool (WSL being the acronym for the Swiss Federal Institute for Forest, Snow and Landscape Research). This tool has been demonstrated to have utility for evaluating landscape change in mountainous topography (Steiner, 2011; Wiesmann, Steiner, Pozzi, & Bozzini, 2012), but has not been assessed for its accuracy or utility for analyzing large collections of imagery. The WSL Monoplotting Tool is a software tool that relates each photographic pixel to its real-world latitude, longitude, and elevation.

The georeferencing of oblique angle, terrestrial images developed by Bozzini et al. (2012) and implemented in the WSL Monoplotting Tool follows the photogrammetric monoplotting procedure, which is described in detail in Aumann and Eder (1996), Strausz (2001), and Steiner (2011). The assumption of monoplotting is that the camera, a point on the photograph in two dimensions (2D), and the corresponding point in the real world in three dimensions (3D) all lie in a straight line. This relationship is visually depicted in Fig. 2 and described by the collinearity equation below. The equation's variables are shown in Fig. 2 and described in the following text:

$$x_a - x_0 = -f\,\frac{r_{11}(X_A - X_C) + r_{21}(Y_A - Y_C) + r_{31}(Z_A - Z_C)}{r_{13}(X_A - X_C) + r_{23}(Y_A - Y_C) + r_{33}(Z_A - Z_C)}$$

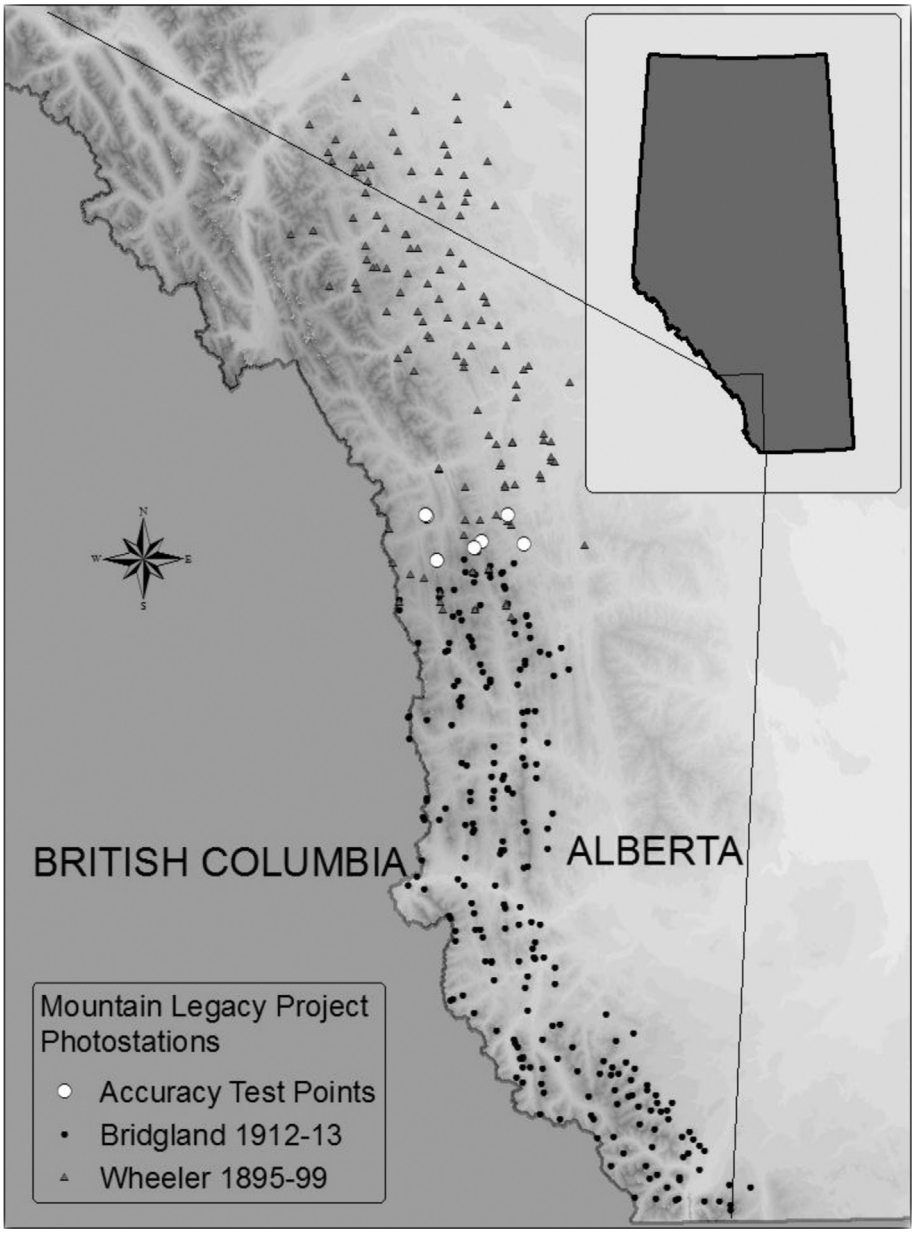

Fig. 1. Location map of Mountain Legacy Project images in the Wheeler 1895–1899 and Bridgland 1913-1914 surveys. Points used in the assessment of the monoplotting tool were chosen from the overlap area between the two surveys. Eight images were used from the six photostations.

$$y_a - y_0 = -f \frac{r_{12}(X_A - X_C) + r_{22}(Y_A - Y_C) + r_{32}(Z_A - Z_C)}{r_{13}(X_A - X_C) + r_{23}(Y_A - Y_C) + r_{33}(Z_A - Z_C)}$$

The values $r_{11} - r_{33}$ are functions of the rotation angles of the camera about the X, Y and Z axes. The value x_0y_0 is the 2D coordinate of the line drawn from the projection center of the camera through the center of the image, and f is the focal length of the camera.

The WSL Monoplotting Tool contains a routine which computes the values of the collinearity equation and determines the external (extrinsic) and internal (intrinsic) camera parameters. This routine starts from a set of five or more control points (CPs) whose correspondence between the 2D oblique image and the 3D real world is well known.

Once the collinearity equation has been solved, vector data (polygon, polyline or point) can be extracted from the image, and exported to a GIS for analysis. In addition to supporting the export of spatially referenced vector data to a GIS, spatially referenced vector data can also be imported to the WSL Monoplotting Tool, and overlain on the photograph. The WSL Monoplotting Tool has been designed for vector data, which is suitable for analysis of a small number of images, or for extracting data from only a portion of an image. To evaluate large landscapes it is considerably more efficient to classify vegetation on a grid or raster basis: by doing so we can take advantage of image classification techniques common in remote sensing. The WSL Monoplotting Tool's utility can be expanded by pairing it with GIS functionality in ArcGIS (or another GIS). We can create a workflow permitting manual or automated image classification (Jean et al. 2015) of oblique angle images and to translate the data into a raster format.

Our objectives were:

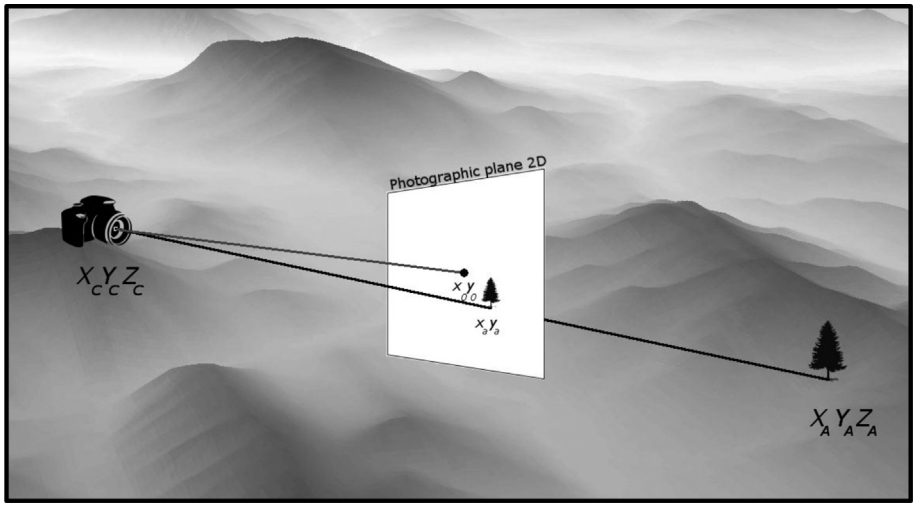

Fig. 2. The collinearity condition as illustrated by the relationship between the camera, and an object with pixel coordinates $x_a y_a$ in the 2D photographic plane, its real world 3D coordinates $X_A Y_A Z_A$. $X_C Y_C Z_C$ indicates the location of the camera position in 3D space.

1) To conduct an assessment of the accuracy of the WSL Monoplotting Tool for georeferencing and extracting vector data from oblique landscape images.
2) Establish a procedure for classifying raster data from oblique photographs using the WSL Monoplotting Tool. While the tool has been designed to extract vector data (polygons, lines and points), manual vegetation classification of images by drawing polygons is a labor intensive process, and there are advantages to using a raster/grid-based classification scheme.

2. Methods

The WSL Monoplotting Tool requires a photograph(s) to be analyzed, a digital elevation model (DEM) of the area visible in the photograph, and control points (extracted from orthophotos, maps or field data). Often for studies involving oblique photographs the use of field data to establish control points is impractical due to the time and cost required to physically visit the locations contained within the images and measure control points using GPS devices. Thus, we established control points by matching features in the oblique photograph with orthophotos of the area. High resolution bare earth DEMs derived from 1 m LIDAR data were made available from the Province of Alberta Ministry of Environment and Sustainable Resource Development (AESRD), as were orthophotos with a resolution of 0.5 m per pixel. Because the orthophotos were recent (2005–2008), we used only the recent (repeat) images from the Mountain Legacy Project photograph collection in this assessment of the accuracy of the WSL Monoplotting Tool (to ensure greater accuracy in placement of the control points). Eight images in total were chosen from the Wheeler Irrigation Survey collection (original images were taken between 1895 and 1899, repeats from between 2007 and 2009) and the Bridgland 1913-1914 Survey (original images were taken between 1913 and 1914, repeats from between 2005 and 2009). The photostation locations for all Wheeler and Bridgland surveys are displayed in Fig. 1. An example of a historic repeat photo pair is shown in Fig. 3A and D.

2.1. Accuracy test

From the field data collected by the MLP photography crews, the location of each photostation was recorded in UTM coordinates, and the approximate azimuth for each photograph is known. A two by two array of DEM tiles (each equivalent to a Canadian National Topographic System 1:20,000 map sheet) was loaded, and for each image within this extent, the ArcGIS 10.2.2 Viewshed tool was run to determine each image's approximate field of view (FOV). From these images, eight were chosen so that there was minimal overlap between any image FOVs (two images shared a small portion of each other's FOV). These eight MLP images taken in 2009 were selected from six photostation locations (two photostation locations were represented by two images each) (Fig. 4). Orthophotos supplied by AESRD were taken in 2007, which greater facilitated identification of features for use as control points. Each image was divided into three horizontal segments (foreground, midground, background) and three vertical segments (left, center, right), for a total of nine segments. Within each segment two to three easily identifiable features were identified as control points. These 21–27 control points in each image were established by matching features visible in the oblique angle photograph and in the corresponding orthophoto. Objects chosen were isolated trees, boulders, road intersections, and other easily recognized features. These control points were distributed throughout the image in the fore-, mid- and background, and from one side to the other. Control points were marked on each MLP image in the GNU Image Manipulation Program (GIMP version 2.8.4), and the orthophotos and DEMs were examined in ArcGIS 10.2.2. The UTM coordinates (latitude, longitude and elevation) of each control point were recorded in a table. These control points were used for georeferencing the images, and for testing the accuracy of the georeferenced outputs created by the WSL Monoplotting Tool.

In theory, if the control points could be precisely placed in both 2D and 3D space, the DEM was a perfect representation of the real world, and there were no lens or sensor/film distortion in the camera, there would be no error in object placement after georeferencing the image. However, DEMs are rarely perfect models of the real world, pixelation in both the 2D images and the orthophotos from which the 3D location is derived cause errors in the placement of features, and camera lenses and sensors/film are rarely perfect.

Fig. 5 shows how these sources of uncertainty affect the accuracy of object placement using the monoplotting principle. There is nearly always some deviation between the ray from the center of the camera through the points identified by the user on the image

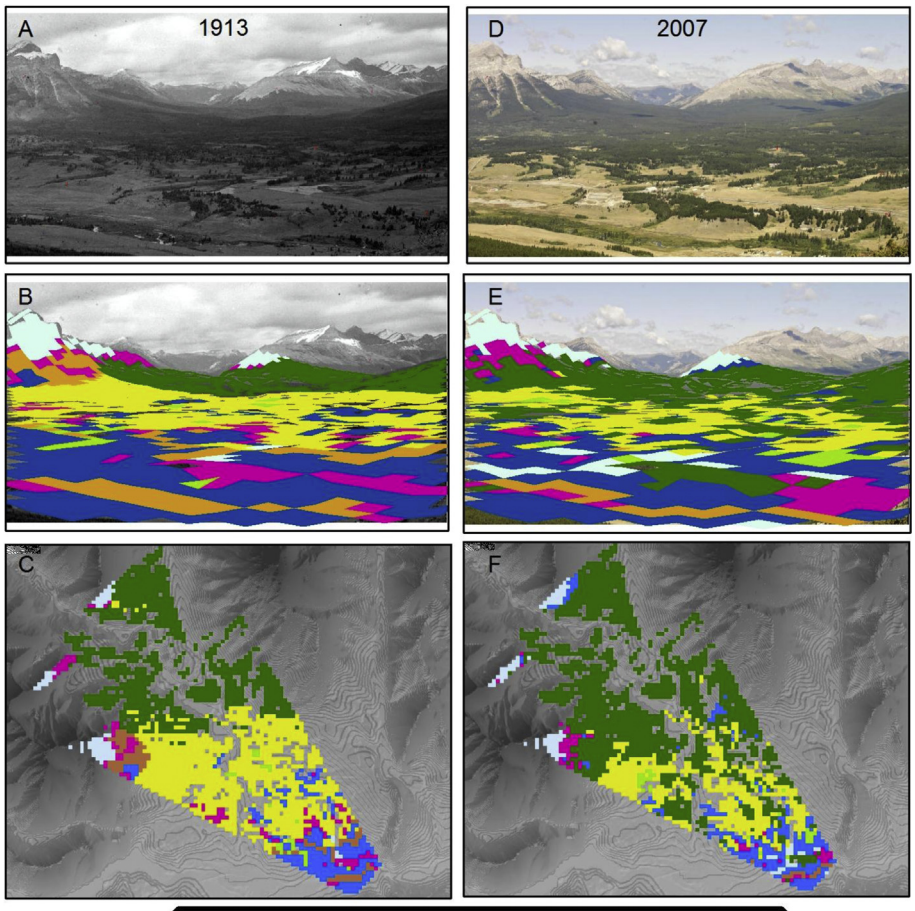

Vegetation Class	1913 (ha)	2007 (ha)	Change
Conifer	842	1409	+567
Broadleaf	33	36	+3
Meadow/Grassland	292	291	-1
Mixedwood	926	488	-438
Non-Vegetated	78	116	+38
Shrub	125	19	-106
Woodland	130	67	-63
Total	2426	2426	

Fig. 3. Mountain Legacy Project image pair (A, D). The original image is from 1913, and the repeat image from 2007. Panels B and E show the change in vegetation classes in the oblique view, and C and F show the orthogonally transformed view. Each grid cell is 100 m × 100 m (1 ha). The attached table shows the total (hectares) of each vegetation category at each time and the total change.

(p') and the DEM (P'), and the ray that aligns camera, and the real points on the image (p) and in the real world (P). If there is no error, the angle between these rays is zero, but this angle of error increases as the points become less accurately placed. The WSL Monoplotting Tool calculates the angle of the deviation between the rays rP' and rP.

For each control point $\boldsymbol{P_c}$ ($\boldsymbol{p}$, $\boldsymbol{P}$) the following data are computed (see Fig. 5 for each parameter represented pictorially):

O, "Origin", or position of the camera (in real world coordinates), $X_cY_cZ_c$ in the collinearity equation and Fig. 2.
P, given point on the image, $x_a y_a$ in collinearity equation and Fig. 2.
P, given point in the world (real world coordinates), $X_AY_AZ_A$ in collinearity equation and Fig. 2.
π, 2D image plane.
π_P, plane through P, perpendicular to the ray r_P
p', projection of P on π (pixel point computed from the real world point P) as a result of displacement of P to P'.
P', reprojection of p on the DEM (real world point computed from the pixel point p) as a result of displacement of p to p'.
P'', projection of P' on π_P
r_P, given ray OpP
$r_{P'}$, computed ray $Op'P'$
d, distance between p and p'
R, distance between P and P''
D, distance between P and P'
$\alpha(r_P, r_{P'})$, angle between r_P and $r_{P'}$

For each image to be georeferenced, all 21–27 control points established on that image were initially selected to compute the intrinsic parameters of the camera. Control points used in the computation routine to solve the intrinsic camera parameters are referred to as Registration Points. Once the intrinsic parameters were computed, for practical reasons the three least accurate

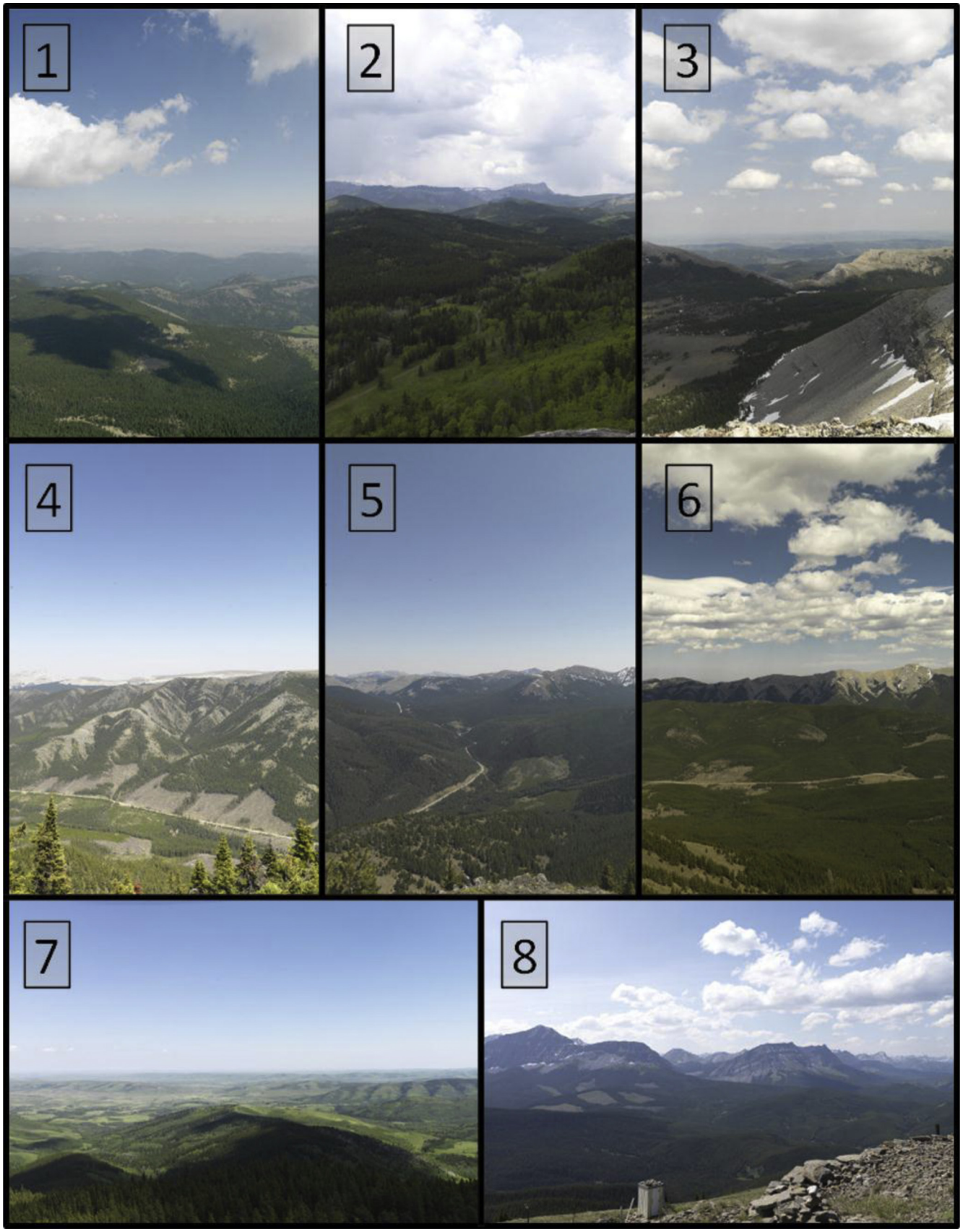

Fig. 4. Mountain Legacy Project images used in testing the accuracy of the WSL Digital Monoplotting Tool. All images are from Higgs et al. (2009).

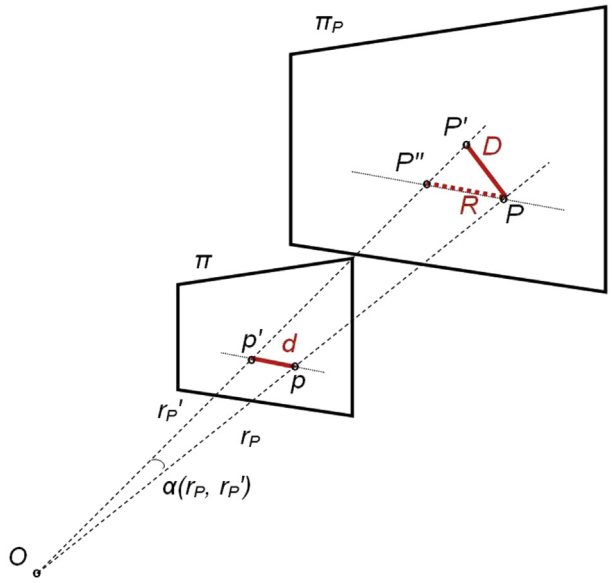

Fig. 5. The difference between the modeled relationship and the real relationship between objects in the real world (3D) and the photographic plane (2D). Ray O*pP* (r*P*) aligns the camera, the image point *p*, and the real world object *P*. Ray O*p*′*P*′ shows the computed line due to errors arising from control point placement, lens distortion, sensor/film distortion, DEM inaccuracies, or any combination of these factors. If image point *p* is misplaced by the user at *p*′, the real world point *P* is then projected to *P*′. Conversely, if the real world point *P* is displaced at *P*′, then image point *p* gets projected at *p*′. Errors in the placement of both *p* and *P* compound the displacement.

registration points – as indicated by the "angle error" described above ($\alpha(r_P, r_P')$) – were dropped, and the intrinsic parameters of the camera were then recalculated using the reduced number of registration points. This procedure was repeated iteratively, dropping the three least accurate registration points, then recomputing the parameters of the camera on the reduced number of registration points until the "best" six registration points remained. For example, if an image had 21 control points identified, we calculated the camera parameters first using 21 registration points, then 18, 15, 12, 9, and finally 6. For each image, these remaining six registration points and the resulting intrinsic camera parameters defined the "best camera" solution. To assess the sensitivity of the WSL Monoplotting Tool to the accuracy of control point placement, we also created "worst camera" and "random dispersed camera" solutions. The least accurate six registration points as defined by $\alpha(r_P, r_P')$ (the first two sets of three control points dropped in the "best camera" solution) were used to create a "worst camera" solution. Additionally, six evenly dispersed semi-randomly chosen registration points were used to create a "random-dispersed" camera solution.

These three different camera solutions (best, worst and random-dispersed) were developed for each image to compare the accuracy of the WSL Monoplotting Tool in reprojecting the remaining control points (ie. non-registration points). The discarded control points from each image's best-, worst- and random dispersed-camera solutions were then used as test points to determine how accurately they would be reprojected on the DEM using the WSL Monoplotting Point tool. These test points were drawn on the images in the WSL Monoplotting Tool and the spatially referenced points exported to ArcGIS. Some points had to be excluded from the analysis. The excluded points were all situated at the top of hills and ridges with highly oblique angles of viewing incidence (see Fig. 6) from the observation point to the control point location. The small amounts of error in the angle these object were placed at resulted in the points being displaced either above the horizon (an infinite distance away), or a large distance away on ridges behind the correct one.

Several different metrics were calculated to assess the accuracy of the WSL Monoplotting Tool intrinsic camera parameters computed for each image. Table 1 shows all computed values associated with the error testing. These computed values for each image and its best-, worst- and random-dispersed internal camera solutions are as follows:

- *Error vector length* (per point): Parameter *D* in Fig. 5. The distance between the reprojected Test Point (*P*′) and actual Control Point (P) location was measured by creating new line features in ArcGIS, and computing the length of the line.
- *Mean error vector length* (per image–camera combination): for all test points in each image-intrinsic camera solution, the mean error vector length was calculated (arithmetic mean of all *D* per image–camera combination).
- *Angle of viewing incidence* (per point): using a ray from the camera location to each control point the angle between the viewing vector and the mean slope/aspect of a 10 m segment of the line running from the camera through the control point and fixed to the ground. See Fig. 6.
- *Displacement error* (per image–camera combination): the geometric centre (centroid) of all Test Points (*P*′) and Control Points (*P*) for each image–camera combination was computed, and the difference between these centroids is the Displacement Error for each image–camera combination. Additionally, the geometric center for all Test Points (*P*′) and Control Points (*P*) was calculated for each camera solution (all images combined) to determine the total landscape displacement error.

To determine whether the mean vector length (errors in object placement) is a function of the angle of incidence, or the distance from the camera a General Linear Model was constructed in SPSS version 21 as:

$$\begin{aligned}\text{Vector length error (meters)} = \text{Intercept} \\ + \beta * \text{Image (random factor)} \\ + \beta * \text{Distance to camera} \\ + \beta * \text{Angle of viewing incidence.}\end{aligned}$$

2.2. Extracting raster data

To extract raster data from images, a new system was developed and demonstrated using a single image taken in 2006 (Fig. 7). The image was georeferenced using a best camera solution (as described above). With the X, Y, and Z coordinates of the origin (camera placement) derived from the WSL Monoplotting Tool, a viewshed analysis (ArcGIS 10.2.2) was conducted. The FOV was limited to the horizontal angle of the camera's field of view (parameters Azimuth1 and Azimuth2 of the ArcGIS Viewshed tool) by measuring the azimuths of left and right edges of the image (calculated in the WSL Monoplotting Tool using the Viewshed Parameters export function). The nearest and farthest edge of the FOV (parameters Radius1 and Radius2 of the ArcGIS Viewshed tool) were determined by placing points in the WSL Monoplotting Tool at the nearest edge and in the distance at a point beyond which the images become so pixelated that classification of vegetation is difficult. This FOV was calculated using the 1 m resolution DEM used in all the above procedures. The Fishnet tool (ArcGIS 10.2.2)

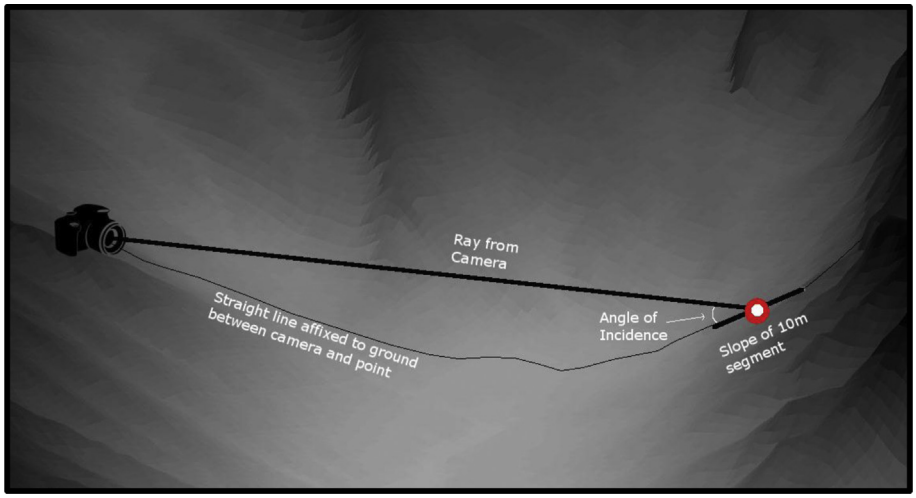

Fig. 6. The angle of viewing incidence between the ray from the camera (r_P), and the slope of a 10 m line segment from a line between the camera and point *P* affixed to the ground. Lower angles of incidence increase the 3D distance between *P* and *P′*.

Table 1
Measurement of errors in monoplotting procedure using eight Mountain Legacy Project images.

Image	Camera solution	# registration points	# test points	Mean angle error	Mean angle of viewing incidence (range)	Mean error vector length (m) *D* (+/− SE)	Mean displacement error (m)
1	Best	6	15	.007	21.3° (9.3–32.6)	4.7 (.7)	1.7
	Random-dispersed	6	15	.027		5.9 (1.0)	1.9
	Worst	6	15	.041		14.8 (3.0)	7.1
2	Best	6	15	.002	21.3° (5.7–36.4)	8.3 (1.8)	1.9
	Random-dispersed	6	15	.028		18.1 (4.0)	9.5
	Worst	6	12	.115		61.6 (12.6)	55.4
3	Best	6	15	.007	18.9° (7.0–36.5	11.7 (2.6)	2.0
	Random-dispersed	6	16	.038		10.7 (2.6)	2.3
	Worst	6	16	.218		24.8 (3.6)	11.1
4	Best	6	15	.013	27.3° (4.9–48.6)	16.0 (6.2)	4.8
	Random-dispersed	6	15	.085		25.8 (7.6)	6.9
	Worst	6	14	.199		10.5 (2.4)	6.3
5	Best	6	16	.003	25.8° (3.6–47.9)	10.2 (3.0)	4.3
	Random-dispersed	6	14	.034		12.3 (4.2)	7.8
	Worst	6	16	.067		72.1 (16.7)	38.7
6	Best	6	18	.003	28.3° (2.4–51.8)	7.8 (1.6)	1.9
	Random-dispersed	6	19	.016		9.3 (1.8)	0.8
	Worst	6	19	.074		23.3 (3.9)	16.9
7	Best	6	15	.014	14.7° (1.9–38.3)	48.0 (14.9)	26.4
	Random-dispersed	6	15	.220		108.5 (27.0)	35.1
	Worst	6	14	.338		96.2 (24.6)	70.4
8	Best	6	12	.007	20.1°(13.0–43.3)	11.9 (3.5)	9.2
	Random-dispersed	6	12	.034		8.7 (2.5)	7.0
	Worst	6	11	.129		33.4 (8.4)	27.0
Total	Best		121			14.7 (2.4)	2.9
	Random-dispersed		121			24.8 (4.5)	5.0
	Worst		117			41.2 (4.8)	9.1

was used to create a 100 m * 100 m grid across the landscape contained within the image, and this fishnet grid was intersected with the FOV to isolate the grid cells visible within the images. Cells that had less than 75% visibility were excluded to avoid making assumptions about the content of the invisible portion of the cell. This 100 m grid was then transformed from the orthogonal perspective (world coordinates) to the oblique perspective (pixel coordinates) using the WSL Monoplotting Tool's World Shapefile to Pixel Shapefile tool. This perspective-transformed grid was then overlain on the image in ArcGIS. In each grid cell, the vegetation was manually classified as either a) grass, b) shrub, c) open woodland, d) broadleaf, e) mixedwood, or f) coniferous forest cover. The classified oblique perspective grid cells were transformed back to the orthogonal perspective by using the Pixel Shapefile to World Shapefile tool of the WSL Monoplotting Tool. This fishnet grid was then converted to raster coverage, thereby completing the process of classifying the vegetation visible in the oblique image and converting it to orthogonal perspective raster data ready for summary and analysis in a GIS. This process of georeferencing, overlaying a grid, and interpreting vegetation to a raster coverage was repeated with the original photograph (taken in 1913), and the change in vegetation over 94 years is displayed in Fig. 3.

3. Results

With the available data inputs the WSL Monoplotting Tool had a mean vector length error of 14.7 m (s.e. 2.4 m) when using the best-camera solution to georeference the image (see Table 1 for all

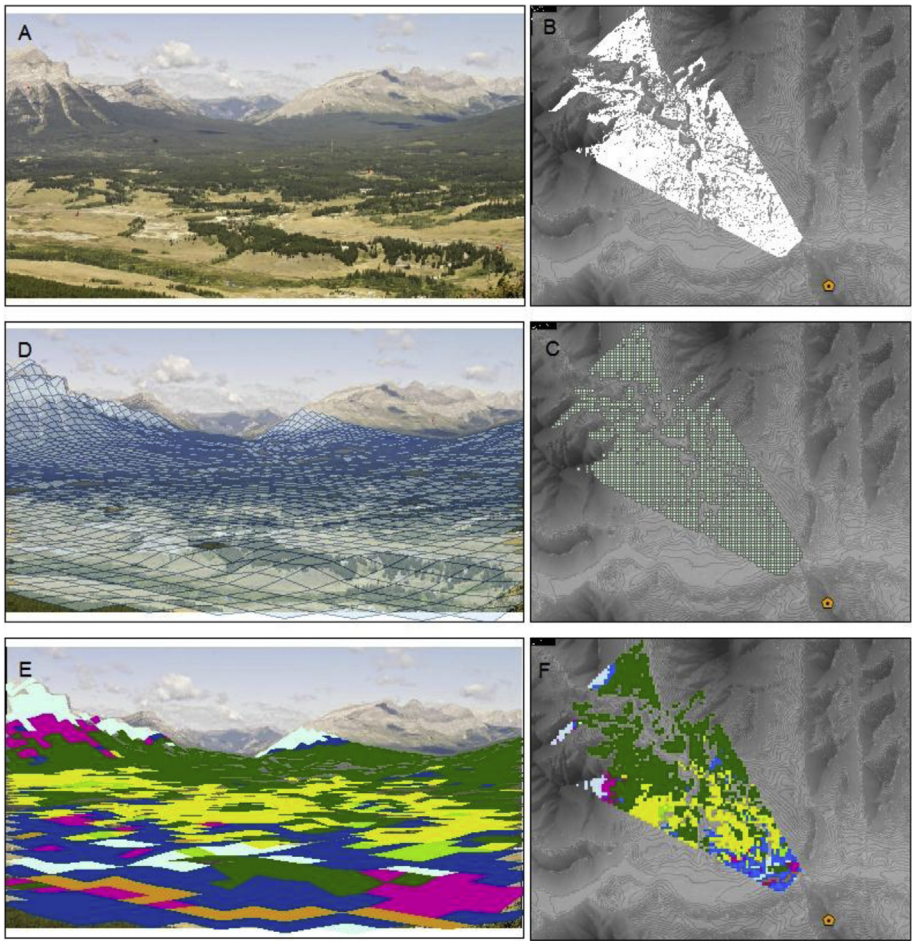

Fig. 7. Procedure for raster analysis of oblique images using the WSL Monoplotting Tool. A) Image to be analyzed, B) Viewshed of image after georeferencing to identify photo origin, C) 100 m × 100 m fishnet grid intersection with the viewshed, D) oblique perspective of fishnet grid overlain on image, E) classified vegetation on image F) orthogonal transformation and spatially referenced classified grid cells. 2 column image.

accuracy and error values). The worst-camera solution yielded a mean error vector of 41.2 m (s.e. 4.8 m). For the random-dispersed camera solution this measurement error was 24.8 m (s.e. 4.5 m). When considering the mean displacement error (the geographic centre of all points measured) the measurement error was reduced to 2.9 m (best camera), 5.0 m (random-dispersed camera), and 9.1 m (worst-camera).

The effect of distance to camera and angle of viewing incidence variables on the vector length error were significant at $\alpha = 0.05$. Using all 121 test points, the General Linear Model yielded the equation:

$$\begin{aligned}\text{Error vector length (meters)} = {} & 12.1 + \beta\text{*Image} \\ & + .003\text{*(Distance to camera)} \\ & - 0.596\text{*(Angle of viewing incidence)}\end{aligned}.$$

Using the methods described above to extract raster data from images in the WSL Monoplotting Tool, Fig. 7 shows an image a) that has been georeferenced using the WSL Monoplotting Tool, b) a viewshed calculated, c) a spatial grid intersected with the viewshed and d) transformed to the oblique perspective and overlain on the image, e) the vegetation in the image classified, and f) retransformed back to the orthogonal perspective for analysis in a GIS. Fig. 3 shows the same image (3D), its original paired image (3A) from 1913, the classified vegetation in both images (3B, C, E, F), and a summary of the changes in vegetation cover between the two time periods.

4. Discussion

The Mountain Legacy Project notwithstanding, there are many historical repeat photograph collections available showing landscape change in many regions of the world. Literature and internet searches of the terms “historical repeat photography” yield a large number of different studies, collections, and publications. However, as has been described in the introduction of this paper, these studies have been primarily limited to qualitative or relative comparisons of change (Hastings & Turner, 1965; Gruell, 1980, 1983; Webb, 1996). In the limited number of studies that have managed to spatially evaluate changes, they were limited to studying very small areas of the landscape due to the complexity of the analytical methods available (Rhemtulla et al. 2002; Corripio, 2004; Watt-Gremm, 2007; Roush et al., 2007), and the accuracy of the spatial data outputs is unknown. There are a few studies that have used this new WSL Monoplotting Tool (Steiner, 2011; Wiesmann et al. 2012; Bozzini et al. 2012), but they have only extracted vector data. While these are spatially accurate, they too have only looked at limited spatial scales. To be of value in management applications, imagery showing change is most useful when:

a) it can be described and quantified
b) is spatial and accurate
c) assessment procedures are rapid to facilitate landscape-scale analysis.

In this paper, we have not only used the WSL Monoplotting Tool to georeference and extract classified vector data to assess the spatial accuracy of the tool, we have developed a new approach to extract raster data from oblique angle images. This raster-based approach will permit researchers to evaluate large image collections, and has the potential to be combined with automated image classification techniques common in the field of remote sensing. This adds considerable value to the multitude of repeat photography projects that have been conducted, are in progress today, or will be conducted in the future. These new techniques create the potential to expand the field of remote sensing to a much wider user audience and array of data sources. Oblique-angle land-based imagery is a widely available data source, but until recently has not been useable for quantitative spatial analysis. While repeat land-based photography has been used as a data source in many assessments of landscape change, researchers have been restricted to qualitative or relative comparisons of change over time, or have been restricted to quantitative analysis of very small areas.

The value of historical repeat photography to document ecological change has long been recognized (Pickard, 2002; Webb, Boyer, & Turner, 2010), primarily because it extends the temporal scale we can study. Aerial photography is temporally limited to the early to mid 20th century, whereas land based photographs exist into the late 19th century. While extending the temporal record by roughly 50 years may seem trivial for some lines of inquiry, it extends our window of photographic observation to the beginning of the European settlement era in western North America, South America, New Zealand and Australia, and other parts of the world. In all parts of the world, the beginning of the 20th century was a time when considerable change was occurring on the landscape, as this coincided with a period of rapid population growth and technological advancement. While it is our objective to evaluate landscape scale vegetation change using historical photography, there are many other potential uses of historical imagery. Paired historical photographs can show changes in glaciation, river channels, shorelines, erosion, land use, architecture, settlements, and many other things.

The value in being able to spatially quantify things visible in oblique angle terrestrial photographs is not only restricted to studying historical change predating the era of aerial photography. Even when the temporal period of interest is covered by aerial imagery, it is often not readily accessible, and can be expensive to acquire new imagery. Land based photographs are ubiquitous and considerably less expensive to obtain. Furthermore, terrestrial based oblique angle imagery can be useful without being paired to historical imagery. Provided the data inputs outlined in this paper are available (a DEM and some control points), any photograph can be georeferenced and spatial data can be extracted from it.

As we have demonstrated, the WSL Monoplotting Tool is effective for georeferencing oblique angle photographs. With the built in functionality to georeference the image and import and export spatial data, and with tools designed to work with ArcGIS (Viewshed Parameters) and other GIS software, the WSL Monoplotting Tool allows users to accurately and rapidly analyze many images. It is currently being used by the authors of this paper to evaluate landscape level change visible in roughly 150 photo pairs from the Mountain Legacy Project covering approximately 350,000 ha.

The accuracy of the WSL Monoplotting Tool is limited by the mensuration or placement of the control points on the image itself and on the DEM, which is largely a function of the resolution of the images at hand (both the photograph being analyzed and the orthophotos being used to find the control point locations). It can also be limited by inaccuracies in the DEM, or lens distortion of the camera itself. The influence of distance to the camera on vector length error factor is mainly due to the difficulty in accurately placing control points on the image when they are farther from the camera (due to the high degree of pixelation that occurs when zooming in). Caution should be exercised when interpreting features that are at low angles of incidence and close to terrain breaks, where slight errors in angles can result in large horizontal displacement. Control points should not be placed in the following locations:

- On surfaces that have a very low angle of viewing incidence,
- On tops of hills/ridges/terrain breaks where there is a risk they could be displaced by very long distances.
- Further away than the most distance objects to be classified (i.e., if limiting analysis to within 5 km of the camera, control points should be placed within 5 km).

While the WSL Monoplotting Tool was not designed to extract or work with raster data, we have herein demonstrated that a workflow can be created that expands the functionality of the tool. The advantage to interpreting vegetation as raster rather than polygon is that a larger number of images can be analyzed, and larger landscape level inferences can be made. The resolution of the raster grid size should be considerably greater than the error in georeferencing accuracy to ensure that classification of the grid cell is spatially correct. If the recommendations regarding control point placement are followed, the errors in georeferencing can be minimized considerably.

With the growing interest in using historical photography, and with recent advancements in computing power, the WSL Monoplotting Tool, in conjunction with GIS software, high resolution DEMs and orthophotos can be used to accurately georeference and classify land based photographs to document and quantify ecological change over a longer time period than that afforded by aerial imagery.

Acknowledgments

This research has been made possible by funding from the Natural Sciences and Engineering Research Council of Canada (NSERC) Post Graduate Scholarship – Doctoral Award, Alberta Innovates Technology Futures Graduate Student Scholarship, and scholarships from the University of Alberta Graduate Student Association (President's Award, Queen Elizabeth II, William McCardell Memorial Scholarship).

I would like to thank the following individuals for their contributions and inspiration: Graham Watt, Catherine Boyes, Caitlin Mader, and Margaret Raiman.

References

Agee, J. K. (1998). The landscape ecology of western forest fire regimes. *Northwest Science, 72*, 24–34.

Arno, S. F., & Gruell, G. E. (1983). Fire history at the forest-grassland ecotone in southwestern Montana. *Journal of Range Management, 36*(3), 332.

Arno, S. F., Parsons, D. J., & Keane, R. E. (2000). Mixed severity fire regimes in the Northern Rocky Mountains: consequences of fire exclusion and options for the future. *USDA Forest Service Proceedings Rocky Mountain Research Station, 5*, 225–232.

Aschenwald, J., Leichter, K., Tasser, E., & Tappeiner, U. (2001). Spatio-temporal landscape analysis in mountainous terrain by means of small format photography: a methodological approach. *IEEE Transactions Geoscience Remote Sensing, 39*(4), 885–893.

Aumann, G., & Eder, K. (1996). An integrated system of digital monoplotting and

DTM modelling for forestry applications. *International Archives of Photogrammetry and Remote Sensing, 31*(B7), 221–225.
Baker, W. L. (1992). Effects of settlement and fire suppression on landscape structure. *Ecology, 73*(5), 1879–1887.
Bozzini, C., Conedera, M., & Krebs, P. (2012). A new monoplotting tool to extract georeferenced vector data and orthorectified raster data from oblique non-metric photographs. *International Journal of Heritage in the Digital Era, 1*(3), 499–518.
Corripio, J. G. (2004). Snow surface albedo estimation using terrestrial photography. *International Journal of Remote Sensing, 25*(24), 5705–5729.
Fluehler, M., Niederoest, J., & Akca, D. (2005). Development of an education software system for the digital monoplotting. In *Proceedings of the ISPRS workshop tools and techniques for e-Learning, Potsdam, Germany, June 1–3, 2005* (On CD-ROM).
Gruell, G. E. (1980). *Fire's influence on wildlife habitat on the Bridger-Teton National Forest, Wyoming – Volume I: Photographic record and analysis*. USDA Forest Service, Intermountain Forest and Range Experiment Station. INT-235:1–207.
Gruell, G. E. (1983). *Fire and vegetative trends. In the northern rockies: Interpretations from 1871–1982 photographs*. USDA General Technical Report, INT-158:1–117.
Hastings, J. R., & Turner, R. M. (1965). *The changing mile. An ecological study of vegetation change with time in the lower mile of an arid and semiarid region*. University of Arizona Press.
Higgs, E., Bartley, G., & Fisher, A. (2009). *The Mountain Legacy Project* (2nd ed., p. 80). University of Victoria Press.
Higgs, E. S., Falk, D. A., Guerrini, A., Hall, M., Harris, J. A., Hobbs, R. J., et al. (2014). The changing role of history in restoration ecology. *Frontiers in Ecology and the Environment, 12*(9), 499–506.
Jean, F. A., Branzan Albu, D., Capson, D., Higgs, E., Fisher, J. T., & Starzomski, B. M. (2015). The mountain habitats segmentation and change detection dataset. In *Proceedings of the IEEE Winter Conference on Applications of Computer Vision (WACV), Waikoloa Beach, HI, USA, January 6–9, 2015*.
Manier, D., & Laven, R. (2002). Changes in landscape patterns associated with the persistence of aspen (Populus Tremuloides Michx.) on the western slope of the Rocky Mountains, Colorado. *Forest Ecology and Management, 167*, 263–284.
Mitishita, E. A., Machado, A. L., Habib, A. F., & Gonçalves, G. (2004). 3D monocular restitution applied to small format digital airphoto and laser scanner data. In *Proceedings of Commission III, XXth ISPRS Congress (International Society for Photogrammetry and Remove sensing), Istanbul (Turkey), July 12–23, 2004. Remote sensing and spatial information sciences* (Vol. 35(B3), pp. 70–75).
Pickard, J. (2002). Assessing vegetation change over a century using repeat photography. *Australian Journal of Botany, 50*, 409–414.
Rhemtulla, J. M., Hall, R. J., Higgs, E. S., & Macdonald, S. E. (2002). Eighty years of change: vegetation in the montane ecoregion of Jasper National Park, Alberta, Canada. *Canadian Journal of Forest Research, 32*(11), 2010–2021.
Romme, W. H., Allen, C. D., Bailey, J. D., Baker, W. L., Bestelmeyer, B. T., Brown, P. M., et al. (2009). Historical and modern disturbance regimes, stand structures, and landscape dynamics in piñon–juniper vegetation of the western United States. *Rangeland Ecology & Management, 62*(3), 203–222.
Roush, W., Munroe, J. S., & Fagre, D. B. (2007). Development of a spatial analysis method using ground-based repeat photography to detect changes in the alpine treeline ecotone, Glacier National Park, Montana, U.S.A. *Arctic, Antarctic, and Alpine Research, 39*(2), 297–308.
Shinneman, D. J., Baker, W. L., Rogers, P. C., & Kulakowski, D. (2013). Fire regimes of quaking aspen in the Mountain West. *Forest Ecology and Management, 299*, 22–34.
Steiner, L. (2011). *Reconstruction of glacier states from geo-referenced historical postcards* (Masters of Science thesis). Zurich, Switzerland: Swiss Federal Institute of Technology.
Strausz, D. A. (2001). An application of photogrammetric techniques to the measurement of historical photographs. In *Class paper for Geography 522: Reconstructing Historic Landscapes*. Oregon State University (Professor Ronald Doel).
Trant, A., Starzomski, B., & Higgs, E. (2015). A publically available database for studying ecological change in mountain ecosystems. *Frontiers in Ecology and the Environment, 13*(4), 187–188.
Watt-Gremm, G. (2007). *Taking a good long look: Disturbance, succession, landscape change and repeat photography in the upper Blakiston Valley, Waterton Lakes National Park*. Victoria, B.C: University of Victoria (Masters of Science thesis).
Webb, R. H. (1996). *A century of environmental change in Grand Canyon: Repeat photography of the 1889–1890 Stanton expedition on the Colorado River*. Tucson: University of Arizona Press.
Webb, R. H., Boyer, D. E., & Turner, R. M. (Eds.). (2010). *Repeat photography: Methods and applications in the natural sciences*. Washington DC, USA: Island Press.
Wiesmann, S., Steiner, L., Pozzi, M., & Bozzini, C. (2012). Reconstructing historical glacier states based on terrestrial oblique photographs. In *Proceedings of AutoCarto 2012, Columbus, OH, USA, September 16–18, 2012*.